Polymer 253 (2022) 124997

Contents lists available at ScienceDirect

Polymer

journal homepage: www.elsevier.com/locate/polymer

Characterization of grafting properties of ABS latexes: ATR-FTIR vs NMR spectroscopy

Ainara Agirre, Miren Aguirre *, Jose R. Leiza **

POLYMAT eta Kimika Aplikatua saila, Kimika Fakultatea, University of the Basque Country (UPV/EHU), Joxe Mari Korta Zentroa, Tolosa Hiribidea 72, 20018, Donostia-San Sebastian, Spain

ARTICLE INFO

Keywords:
ABS polymer
Grafting properties
Grafting characterization
NMR
ATR-FTIR

ABSTRACT

Acrylonitrile–Butadiene–Styrene (ABS) polymers have a complex microstructure which is formed during the grafting reaction of a polybutadiene seed latex. During the reaction, some styrene-acrylonitrile (SAN) chains are grafted onto the polybutadiene (PB) backbone chains, and this grafting is critical to achieve effective dispersion and compatibility of both phases. Therefore, accurate characterization of grafting properties helps understanding the polymerization mechanism as well as the final properties of the ABS polymer and its applications properties. In this work, the grafting properties of ABS latexes were determined by separation of the soluble and insoluble phase of the polymer, followed by the characterization of these phases using analytical techniques. Phase separation was carried out dispersing the latex in acetone followed by ultracentrifugation. The soluble and insoluble polymer phases were for the first time analysed by NMR spectroscopy to obtain the corresponding fractions of SAN and PB in each phase. The soluble fraction was analysed by liquid-state ^{1}H Nuclear Magnetic Resonance (NMR) spectroscopy, whereas the insoluble fraction was analysed by solid-state ^{13}C NMR spectroscopy. Moreover, both phases were analysed by Attenuated Total Reflectance-Fourier Transform Infrared Spectroscopy (ATR-FTIR), and the results obtained are compared and discussed in this article. We found that the most accurate grafting properties are achieved by analysing the composition of the soluble and insoluble fraction by NMR spectroscopy.

1. Introduction

ABS polymers include a large family of resins with excellent toughness, good dimensional stability, good chemical, mechanical and thermal resistance. In addition, altering structural and compositional parameters different properties can be achieved, such as, transparency and flame retardant properties, which can be obtained adding comonomers or additives, respectively, to the final formulation of the polymer. Therefore, the polymer can be customize to meet specific requirements of the products [1].

For instance, in terms of physical properties, a wide range of mechanical and impact properties can be obtained varying different characteristics, such as, comonomer composition, rubber content, degree of crosslinking, grafting properties, particle size and particle size distribution, molecular weight of grafted and rubber polymer and particle morphology, among others [1]. These characteristics are defined during the emulsion polymerization process, hence, the characterization of the microstructure is of high importance to meet the specific properties of the material.

During the grafting reaction, which can be carried out by an emulsion polymerization process, SAN chains are grafted onto the PB backbone chains, but free SAN chains are also formed. In this way, ABS polymer particles with internal particle morphology, as the one schematically showed in Fig. 1, are obtained. The SAN chains can be grafted forming occlusions or clusters (internal grafting), which are dispersed in the PB matrix [2–4]. In addition, SAN chains can be grafted around the PB matrix (external grafting), and the rest of the shell is formed by free SAN chains [2–4]. Therefore, the ABS polymer is composed by a multiphase structure that enables the compatibility between both SAN and PB phases.

Grafting of the SAN onto the PB is critical to achieve effective dispersion and compatibility of both phases, and its accurate determination is of paramount importance for understanding the grafting reaction as well as for its impact in the final microstructure and properties

* Corresponding author.
** Corresponding author.
E-mail addresses: miren.aguirre@ehu.eus (M. Aguirre), jrleiza@ehu.eus (J.R. Leiza).

https://doi.org/10.1016/j.polymer.2022.124997
Received 1 April 2022; Received in revised form 20 May 2022; Accepted 20 May 2022
Available online 24 May 2022

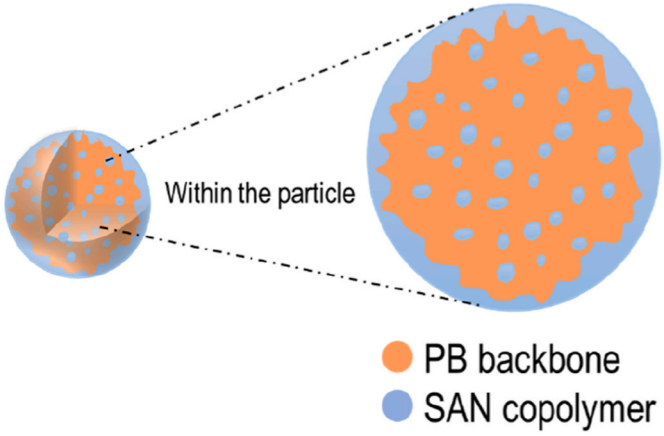

Fig. 1. Scheme of the internal particle morphology of an ABS polymer particle.

of the ABS material. Therefore, characterization of grafting properties can help to determine and quantify the compatibility between these two phases. The characterization of grafting properties involves determination of grafting degree (GD) and grafting efficiency (GE), which can be defined with the following equations:

$$GD\ (\%) = \frac{W\ (\text{grafted SAN})}{W\ (\text{total PB})} \cdot 100 \quad (1)$$

$$GE\ (\%) = \frac{W\ (\text{grafted SAN})}{W\ (\text{grafted SAN}) + W\ (\text{free SAN})} \cdot 100 \quad (2)$$

On the one hand, GD can be defined as the mass of grafted SAN copolymer with respect to the total mass of PB present in the sample. On the other hand, GE can be defined as the mass of grafted SAN copolymer with respect to the total SAN polymerized, both grafted and free SAN chains.

In the literature [2–19], the grafting properties of ABS polymer have been determined by different methods that in most of the cases consists of two main steps. The first step is based on the extraction of the soluble phase of the polymer using a selective solvent. Once the separation of the soluble and insoluble phase of the ABS polymer is done, which are considered in the literature as free SAN chains and grafted SAN-g-PB polymer, respectively, the fraction of each phase in the sample is gravimetrically calculated. Then, two approaches are presented to determine the GD and the GE. In one approach, the fraction of the soluble or insoluble phase in the sample is combined with theoretical values taken from the formulation to calculate the grafting properties. The other alternative is to carry out the characterization of either the soluble or insoluble phase by means of analytical techniques, to obtain the fractions of SAN and PB. Then, combining these values with the fraction of the soluble and insoluble phases, previously obtained from the extraction, the grafting properties are calculated. Some authors have performed the characterization of the insoluble phase of the polymer, however, as far as we know, there are no reports were both phases have been characterized. Although AcOH has been the most common solvent, other organic solvents, such as Xylene, Cyclohexane or Methyl Ethyl Ketone (MEK), have also been reported to carry out the extraction.

A detailed description of the different methods employed [2–19] in the literature to compute the grafting degree (GD) and grafting efficiency (GE) of ABS polymer is summarized in the supporting information (SI).

Due to the complexity of the ABS microstructure, which consists of a PB matrix internally and externally grafted with SAN copolymer chains (insoluble phase), free SAN chains surrounding the particle, and ungrafted and non-crosslinked PB chains (also soluble in AcOH), the quantitative characterization of both fractions and consequently, the determination of the grafting properties has been a challenge over decades. In this work, a solvent extraction method was applied to separate the grafted and ungrafted polymer phases of ABS polymer latexes by using ultracentrifugation and AcOH as selective solvent. Subsequently, both soluble and insoluble phases were for the first time analysed by NMR spectroscopy to obtain the corresponding fractions of SAN and PB in each phase. The soluble fraction was analysed by liquid-state ^{1}H NMR spectroscopy, whereas the insoluble fraction was analysed by solid-state ^{13}C NMR spectroscopy. Since the characterization method was not only based on the separation method, but was also completed with the composition characterization of the separated phases, the uncertainties due to the differences between the targeted amounts in the formulation and the actual amounts in the analysed sample were minimized. In addition, the same characterization was performed by ATR-FTIR spectroscopy, which has been commonly used in the literature, and the results obtained by both techniques are compared and critically discussed in this article.

2. Experimental

2.1. ABS latexes

Two ABS latexes, R1 and R2, were used in the present characterization study. The composition of the latexes (in terms of the weight fractions of each comonomer; PB, styrene (S) and acrylonitrile (AN)), final particle size and overall conversion are shown in Table 1. The Z-average particle size was determined by Dynamic Light Scattering (DLS) using a Malvern Zetasizer Nano ZS. The sample was prepared by diluting a droplet of latex with deionized water in a disposable cuvette. The measurement was performed at 20 °C and three size measurements per sample were carried out. An average value of the three repeated measurements has been reported in Table 1.

2.2. Ultracentrifugation

The soluble and insoluble phases of the ABS latexes were separated by dispersing the latex in AcOH followed by ultracentrifugation. Free SAN chains and soluble and non-grafted PB chains compose the soluble phase, while insoluble and non-grafted PB chains and SAN grafted PB chains the insoluble one (see Fig. 2 for a schematic drawing of the composition of each phase). AcOH was used as selective solvent and around 750 mg of latex were dispersed in 20 ml of AcOH during 24 h in order to make the extraction. Then, ultracentrifugation at 4 °C and 40 000 rpm for 6 h was carried out to the polymer dispersion. The ultracentrifugation analyses were carried out in a Hitachi Ultracentrifuge model CP-100NX.

Once the ultracentrifugation was performed, the soluble phase was separated from the precipitated phase and it was dried at room temperature during one week. In addition, it was dried at 100 °C in vacuum during one day to ensure the complete evaporation of AcOH. On the other hand, the precipitated phase was dried at room temperature until constant weight was measured.

Table 1
PB, S, AN and non-polymerizable solids (NPS) mass percentage of R1 and R2 ABS latexes used in the study. Conversion (Conv.), Z-average particle size (dp) measured by DLS of the latexes.

	PB (wt %)	S (wt %)	AN (wt %)	NPS (wt %)[a]	Conv. (%)	dp (nm)
R1 latex	49.7	38.2	12.1	1.5	96	154
R2 latex	61.0	29.6	9.4	1.5	97	439

[a] Based on the total formulation. Includes the initiator, surfactant and buffer used in the reaction.

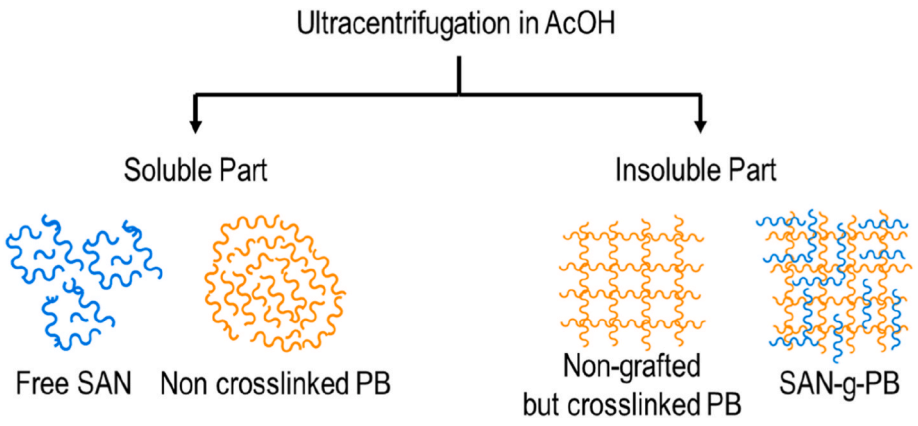

Fig. 2. Expected composition of the soluble and insoluble phase of the ABS polymer obtained by ultracentrifugation in AcOH.

2.3. ATR-FTIR spectroscopy

ATR-FTIR provides information related to the presence of specific functional groups, chemical structures and composition of the polymer. However, if the aim is a quantitative analysis about the composition of the copolymer, a calibration is needed. Therefore, a calibration curve was constructed for each monomer to relate the fraction of the compound to the areas of the spectral bands through Lambert-Beer law, which relates the absorption of the bands to the concentration of the compounds [20]. For the calibration, six latexes of different PB and SAN composition were synthetized by emulsion polymerization, see the details in the SI. Table 2 shows the different composition of these latexes.

For the ATR-FTIR analysis a Nicolet 6700-ATR instruments with Golden gate Harrick accessory was used, and 16 Scans were performed with 4 cm^{-1} of resolution.

2.4. NMR spectroscopy

Soluble and insoluble phases obtained from the separation in the ultracentrifuge were dried and then analysed by NMR spectroscopy. The NMR spectroscopy directly observes the nuclear spins of the atoms or molecules without the need of a calibration to make quantitative analysis. The soluble phase was analysed in the liquid-state NMR, and deuterated DMSO was used as solvent instead of $CDCl_3$ to avoid the superposition of solvent and polymer signals. On the other hand, the insoluble phase was analysed in the solid-state NMR, using few drops of THF. THF was added to the dried samples and the polymer was allowed to swell for 48 before performing the analysis, in order to obtain full mobility of all polymer chains present in the system [21,22].

The liquid-state NMR spectra were recorded on a 500 MHz BRUKER AVANCE-NEO equipped with a BBOF probe. Larmor frequency was 500.13 MHz for ^{1}H nuclei. Relaxation delay was 5 s and the number of scans were 15 160.

The solid-state NMR spectra were recorded on a 9.4T (400 MHz) BRUKER system equipped with a 4 mm MASDVT TRIPLE Resonance HYX MAS probe. Larmor frequency was 100.63 MHz for ^{13}C nuclei. Samples were packed inside 4 mm MAS rotors. Chemical shifts were calibrated indirectly with glycine, carbonyl peak at 176 ppm. Sample rotation frequency was 10 kHz and relaxation delay was 5 s. The number of scans were 8192. High-power SPINAL 64 heteronuclear proton decoupling was applied during acquisition.

Table 2
PB, S and AN mass percentages of polymeric latexes used as calibration standards.

	PB (wt %)	S (wt %)	AN (wt %)
Standard 1	10	68	22
Standard 2	20	60	20
Standard 3	36	49	15
Standard 4	50	38	12
Standard 5	66	26	8
Standard 6	80	15	5

3. Results and discussion

3.1. ABS latexes

Two ABS latexes, R1 and R2, presented in Table 1 were considered for characterization. Latexes with high conversion (see Table 1) and no coagulum were obtained for both R1 and R2 latexes.

The soluble and insoluble phases of the polymer latexes were separated by ultracentrifugation using AcOH as solvent. Table 3 presents the soluble and insoluble fractions obtained for both latexes. The insoluble fraction represents the major part of the polymer in both ABS latexes.

3.2. ATR-FTIR spectroscopy

The ATR-FTIR spectra of the soluble and insoluble phases of the latexes R1 and R2 showed characteristic bands. Fig. 3 is a representative ATR-FTIR spectrum of the soluble phase of the R1 latex with the assignments of the most important bands. The bands wavelength at > 3000 cm^{-1}, 3000 cm^{-1}, 1500-1600 cm^{-1} and 700-750 cm^{-1} correspond to styrene, the one at 2240 cm^{-1} to acrylonitrile and the ones around 900 cm^{-1} to the PB isomers. The remaining spectra for latexes R1 and R2 are presented in Fig. S1 and Fig. S2 of the SI.

One characteristic band corresponding to each polymer (PB, S and AN), which are summarized in Table 4, was used to relate the areas of the absorption bands with the mass percentage of each compound in the sample. Note that the characteristic band of the isomer 1,4-cis-PB overlaps with other styrene deformation band at 700 cm^{-1}. Therefore, using only ATR-FTIR was not possible to determine the composition of the ABS latex and NMR spectroscopy was used to determine the composition of the isomers of the polybutadiene used in the synthesis of the ABS latex.

The three ^{13}C solid-state NMR spectra of polybutadiene seeds S1, S2 and S3 used to produce R1 and R2 latexes can be found in Fig. S3 (SI). The peaks corresponding to each isomer were identified to determine the relation between the 1,4-cis, 1,4-trans and 1,2 PB isomers. This relation was used in the analysis of ATR-FTIR in order to determine the

Table 3
Soluble and insoluble fractions ($Ø_{sol}$ and $Ø_{ins}$) of R1 and R2 ABS latexes.

	$Ø_{sol}$	$Ø_{ins}$
R1 latex	21	**79**
R2 latex	14	86

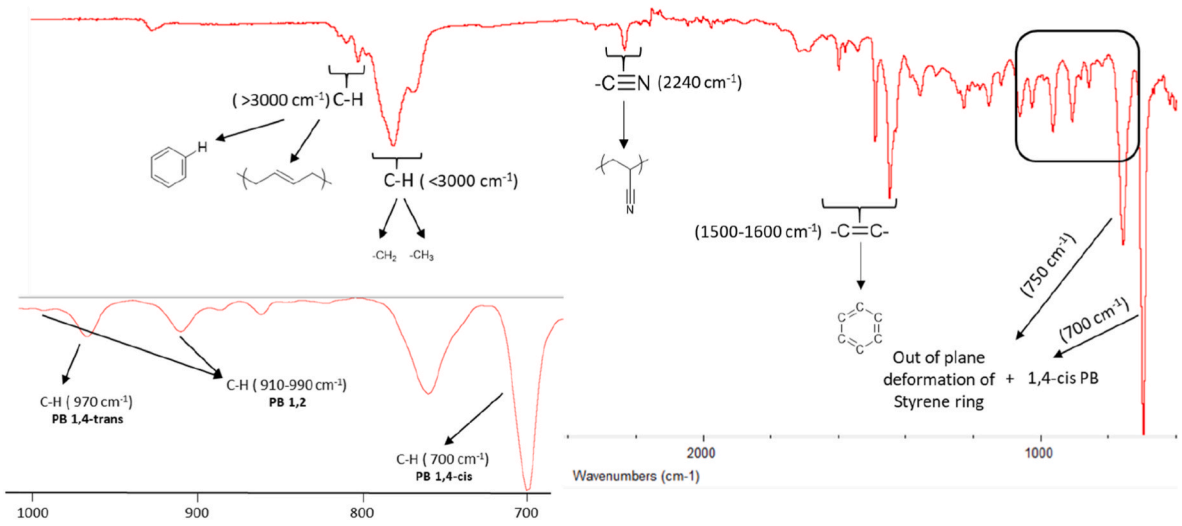

Fig. 3. ATR-FTIR spectrum corresponding to the soluble phase of R1 latex. The spectrum for R2 latex is in the SI.

Table 4
Absorption bands of PB isomers, S and AN in **ATR-FTIR** spectrum.

Polymer	Bond	Absorption band (cm^{-1})
1,4-trans PB	-C – H-	970
1,2 PB	-C – H-	910 and 990
S	aromatic –C = C-	1500–1600
AN	-C≡N-	2240

composition of each compound in the sample.

Table 5 presents the mass percentage of acrylonitrile, styrene and polybutadiene in the soluble and insoluble fractions of latexes R1 and R2. From these values the fractions of SAN and PB in each soluble and insoluble fraction can be easily determined and they are listed in Table 5.

The results indicated that the soluble fractions were rich in SAN (75 and 88% of the soluble fractions, for latex R1 and R2 respectively) and the insoluble fractions were rich in PB (65 and 72% of the insoluble fractions). Since the insoluble fractions of both latexes were around 70% or higher, it can be concluded that most of the SAN copolymer produced was grafted onto polybutadiene chains. It is worth to note that in some of the previous works the soluble phase has been considered exclusively formed by SAN [7–11,18,19], but for the ABS latexes in this work this assumption would introduce a substantial error in the calculation of grafting properties when considering the results obtained by ATR-FTIR technique.

3.3. NMR spectroscopy

To obtain trustworthy and quantitative results in NMR spectroscopy, the spectrum should present both good resolution and sensitivity. It is known that the resolution depends on the mobility of the polymer chains, while the sensitivity is related to the concentration of the sample [22]. As mentioned above, the soluble phase of the polymer was analysed by NMR liquid-state, which presents high resolution due to the solubility of the sample and hence, high mobility of the polymer chains [22,23]. However, the insoluble phase cannot be dissolved in any good solvent (such as, chloroform ($CDCl_3$), DMSO or THF) due to the cross-linking and grafting nature of this polymer fraction; therefore mobility of the chains is limited. In order to characterize the insoluble phase of the polymer, solid-state NMR was used, in which ^{13}C NMR spectra were recorded for quantitative analysis since the ^{1}H spectrum was not suitable for its quantification.

First, the ^{13}C NMR analysis were performed at room temperature and the spectra obtained did not show any peak corresponding to the SAN copolymer. This was attributed to the fact that, ABS polymers have several Tgs, one corresponding to the PB below 0 °C, so at room temperature PB chains have mobility, however, the Tg corresponding to the SAN copolymer is around 100 °C, as a results of which SAN chains have little or no mobility. To overcome the lack of mobility of SAN copolymer chains at room temperature, few drops of THF were added to the ABS samples and allowed to swell for 48 h. The THF allowed swelling and plasticization of the SAN polymer grafted to PB and increase the mobility of the chains making possible to detect the shifts corresponding to SAN, which were elusive at room temperature. This strategy of adding small amount of THF to a sample to be analysed by solid-state NMR was successfully applied to other crosslinked polymer systems previously [21,22].

Fig. 4 shows the ^{1}H NMR spectrum of the soluble fraction of R1 latex. The signal corresponding to the vinylic protons of PB were identified around 5.25 ppm and the signal corresponding to the aromatic protons of S were identified around 6.6–7.5 ppm. The contribution of AN was obtained from the azeotropic relation between the S and AN in the SAN copolymer, which was the composition of the S and AN monomers employed in the feed (S/AN: 76/24 w/w) of the grafting semibatch emulsion polymerizations used to synthesize the analysed ABS latexes. The spectrum of the soluble phase of the latex R2 has the same peaks and it is shown in Fig. S4 in the SI.

Table 5
Mass percentages of each monomer in the soluble and insoluble fractions and weight fractions of SAN and PB in each fraction of R1 and R2 latexes determined by **ATR-FTIR** spectroscopy.

	Fraction	AN (%)	S (%)	PB 1,4 (%)	PB 1,2 (%)	X_{SAN}	X_{PB}
R1 latex	Soluble	18.9 ± 1.7	56.4 ± 1.5	14.6 ± 0.2	10.1 ± 0.2	0.75	0.25
	Insoluble	9.3 ± 1.3	25.9 ± 3.1	50.8 ± 1.1	13.8 ± 0.6	0.35	0.65
R2 latex	Soluble	16.7 ± 0.4	71.6 ± 1.2	7.1 ± 0.3	4.6 ± 0.2	0.88	0.12
	Insoluble	5.6 ± 0.5	22.0 ± 2.6	56.5 ± 1.1	15.6 ± 1.2	0.28	0.72

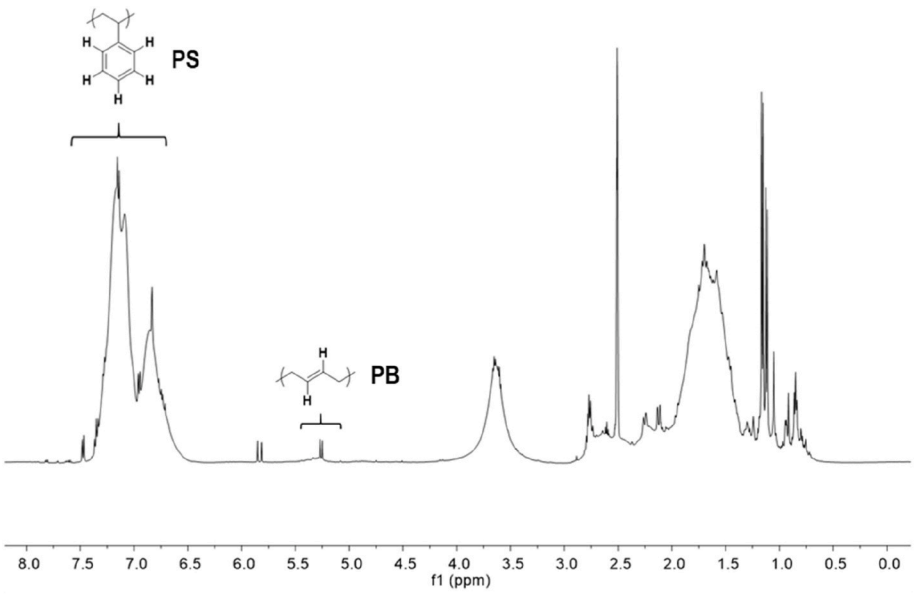

Fig. 4. Liquid-state ^{1}H NMR spectrum of the soluble phase of R1 latex.

Fig. 5 displays the ^{13}C NMR spectrum of the insoluble fraction of latex R1. The signals corresponding to the vinylic carbon of 1,2-PB, the nitrile group of AN and the tertiary carbon of S were identified at 114 ppm, 121 ppm and 144.7 ppm, respectively. The contribution of 1,4-cis-PB and 1,4-trans-PB was obtained from the isomers ratio measured in the PB seeds and it was assumed that this was maintained in the grafting reactions (see Fig. S3 and Table S2 in the SI). The spectrum of the insoluble fraction of R2 latex was similar and it is presented in the SI (Fig. S5).

From the integrals of the characteristic peaks of the ^{1}H and ^{13}C NMR spectra, the fractions of SAN and PB for each phase were calculated and the values are listed in Table 6.

Table 6 agrees well with the trends measured by ATR-FTIR (see Table 5). In other words, both techniques agrees that the soluble fractions were rich in SAN copolymer, but whereas for NMR this fraction is almost pure SAN for ATR-FTIR the amount of PB is substantial (25 and 12 % for R1 and R2 latexes, respectively). For the insoluble fractions, however, the agreement is far better.

The discrepancy in the determination of the SAN and PB fractions of the soluble fraction is likely related with the calibration used for the ATR-FTIR analysis. All the ABS standards used for calibration contained PB amounts higher than 10%, and hence, the region at lower concentrations might not be well covered and consequently, the ATR-FTIR overestimated the amount of PB. Another source for the discrepancy comes from the fact the ATR-FTIR analyses the polymer close to the surface (typical penetration depth of several microns), which in this case might be richer in PB because of the lower energy of this polymer.

Table 6
Fractions of SAN and PB in the soluble and insoluble fractions of ABS latexes R1 and R2 calculated by NMR spectroscopy.

	Fraction	X_{SAN}	X_{PB}
R1 latex	Soluble	0.99	0.01
	Insoluble	0.38	0.62
R2 latex	Soluble	0.99	0.01
	Insoluble	0.31	0.69

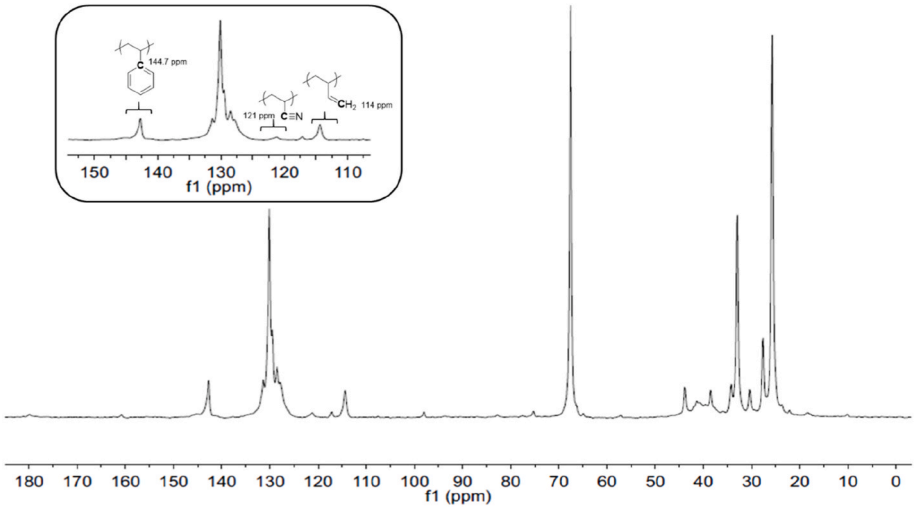

Fig. 5. Solid-state ^{13}C NMR spectrum of the insoluble phase of R1 latex.

3.4. Determination of grafting properties

As it has been explained so far, the SAN and PB fractions, X_{SAN} and X_{PB}, of the soluble and insoluble phase of the polymer were determined by ATR-FTIR and NMR spectroscopies and they are summarized in Tables 5 and 6.

In order to asses if the discrepancy found in the compositions of the soluble fractions was coming from the ATR-FTIR analysis, the total fractions (soluble plus insoluble) of SAN and PB were determined from the data of Tables 5 and 6, and they were compared with the fractions of SAN and PB used in the formulation and the conversion achieved in each polymerization. Table 7 presents the results.

The total SAN and PB fractions obtained by ATR-FTIR method showed a significant difference compared to the composition of the formulation. However, total SAN and PB fractions obtained by the NMR method, were in very good agreement with the formulation employed in both experiments. Therefore, it can be concluded that the error associated with the determination of the composition of the soluble fraction by ATR-FTIR, associated as discussed before with the inaccuracies of the calibration at low PB contents or preferential presence of PB in the surface, makes the analysis by NMR more accurate and robust.

Moreover, using the SAN and PB fractions of the soluble and insoluble phase obtained by ATR-FTIR and NMR spectroscopies, and the masses of the soluble and insoluble phase obtained by ultracentrifugation, the weights needed to determine the GD and GE were calculated using the following equations:

$$W\ (\text{grafted SAN}) = m \cdot Ø\ \text{insol} \cdot X\ (\text{SAN, insol}) \quad (3)$$

$$W\ (\text{free SAN}) = m \cdot Ø\ \text{sol} \cdot X\ (\text{SAN, sol}) \quad (4)$$

$$W\ (\text{insoluble PB}) = m \cdot Ø\ \text{insol} \cdot X\ (\text{PB, insol}) \quad (5)$$

$$W\ (\text{soluble PB}) = m \cdot Ø\ \text{sol} \cdot X(\text{PB, sol}) \quad (6)$$

where m is the total mass of the sample, Ø sol and Ø insol are the soluble and insoluble fractions of the ABS polymer in the sample and X (SAN, sol), X (SAN, insol) and X (PB, sol) and X (PB, insol) are the free SAN fraction in the soluble phase, grafted SAN fraction in the insoluble phase and polybutadiene fraction in the soluble and insoluble phase of the sample, respectively.

With this information and the GD and GE equations presented in the Introduction (Eq (1) and Eq (2)), the grafting properties were calculated and the results for both ABS polymer latexes, R1 and R2, are shown in Table 8.

In an attempt to rationalize the different methods proposed in the literature to calculate GD and GE in ABS latexes, we have compared the results obtained with the more reliable method obtained in this work (which consisted on the separation of the soluble and insoluble phases by ultracentrifugation in AcOH plus the characterization of each fraction by NMR spectroscopy) with the methods used by different authors, discussed in the introduction; namely, we used the equations proposed by the authors and we input the data gathered in this work as indicated below (see Table 9).

In method a) and b), the fraction of the soluble [7–10] or insoluble [2–4,11–16] phase combined with the values taken from the formulation were used to calculate the GD and GE. In the method c) developed by Kuhn et al. [17], the fraction of the insoluble phase of the polymer and the SAN and PB fractions obtained from the characterization of this insoluble phase (by ATR-FTIR spectroscopy) were used to determine the grafting properties. Method d) is the preferred analysis obtained in this work using NMR analysis. The values of GD and GE calculated by the four methods for the two ABS latexes are shown in Table 9.

Table 7
SAN and PB fractions of each latex sample calculated from **ATR.FTIR**, NMR and from the formulation used to synthesize R1 and R2 latexes.

	ATR-FTIR		Formulation		NMR	
	SAN (%)	PB (%)	SAN (%)	PB (%)	SAN (%)	PB (%)
R1 latex	43.8	56.2	50.3	49.7	50.1	49.9
R2 latex	36.7	63.3	39.0	61.0	40.0	60.0

Table 8
GD and GE values obtained by **ATR-FTIR** and NMR methods.

	ATR-FTIR		NMR	
	GD (%)	GE (%)	GD (%)	GE (%)
R1 latex	49.4	63.5	60.1	59.9
R2 latex	37.2	64.2	44.8	67.4

Table 9 presents interesting information regarding the different methods. Method a) and b) are the easiest ones because they only need information of the soluble and insoluble fractions; the rest is taken from the formulation. GD are equal for both methods (note that since Ø sol and Ø insol are obtained from the same experiment *Ø sol =1- Ø insol,* and hence both equations are the same (see legend in Table 9). The calculation of GE differs because method b) accounts for the SAN conversion and the total SAN in the denominator is smaller, leading to higher GE in method b). Method c) [17], does not rely on the formulation to calculate the grafted amount of SAN, but it analyses the composition of the insoluble fraction obtaining a more accurate amount of the SAN grafted to PB (in the literature FTIR was used to determine such composition and hence, here we also used the ATR-FTIR composition). As it can be seen in Table 9, the GE and GD values calculated by method c) are smaller than those calculated my methods a) and b) because the latter, using only information of the formulation, overestimate the amount of grafted SAN, in other words, the fraction of PB in the formulation is smaller than the actual fraction on the insoluble polymer. Method d) differs from method c) in that NMR is used to calculate the composition of the insoluble fraction and to calculate the total amount of polybutadiene in the sample (denominator of GD) and total SAN in the sample (denominator of GE), the values calculated from the compositional analysis of the soluble and insoluble fractions measured by NMR are considered. The GD and GE values obtained by method c), although closer to those of method d), they still present some differences that should be attributed to the lower accuracy on the measurement of the composition of SAN by ATR-FTIR and the use of the formulation to determine the total amounts of PB and SAN in the ABS latexes.

4. Conclusions

The characterization of grafting properties of ABS latexes using NMR spectroscopy has been for the first time performed in this work. In order to obtain the contributions of all the polymer fractions that form the ABS polymer, suitable conditions have been found for both solid-state and liquid-state NMR experiments. The results showed that NMR spectroscopy is more accurate than ATR-FTIR spectroscopy when it comes to quantifying the soluble and insoluble phase of the ABS polymer. NMR technique was able to determine the contributions of the two phases that formed the ABS polymer without the need of a calibration.

In addition, we assessed the methods presented in the literature by comparing the GD and GE calculated in this work for latexes R1 and R2 with the values obtained for the simpler methods that only used the soluble and insoluble fraction plus information from the formulation (methods a and b), and with method c that in addition to the insoluble fraction of the ABS polymer, it measures the composition of this fraction by ATR-FTIR. We found that the simpler methods (a and b) largely overestimate the GE and GD values and preferably should not be used. Method c) provides values that do deviate from the more accurate values obtained with method d) (deviations in the range 0.5–9.5%), but are still reasonable. Due to the fact that method d) is more time consuming that method c) (both the soluble and insoluble phases are analysed by NMR)

Table 9
GD and GE values calculated with the a), b) and c) characterization methods discussed in the literature, and the GD and GE values calculated with the method developed in this work d).

	Method a)		Method b)		Method c)		d) This work	
	GD (%)	GE (%)	GD (%)	GE (%)	GD (%)	GE (%)	GD (%)	GE (%)
R1 latex	70.4	66.6	70.4	68.2	59.8	57.9	60.1	59.9
R2 latex	47.9	73.0	47.9	74.2	40.6	62.8	44.8	67.4

$$\text{a)GD} = \frac{m\cdot[1 - Øsol - Y(PB)]}{m\cdot Y(PB)} \text{GE} = \frac{m\cdot[1 - Øsol - Y(PB)]}{m\cdot[1 - Y(PB) - Y(NPS)]}$$

$$\text{b)GD} = \frac{m\cdot[Øinsol - Y(PB)]}{m\cdot Y(BD)} \text{GE} = \frac{m\cdot[Øinsol - Y(PB)]}{m\cdot Y(SAN)\cdot C}$$

$$\text{c)GD} = \frac{m\cdot Øinsol\cdot X(SAN, insol)}{m\cdot Y(BD)} \text{GE} = \frac{m\cdot Øinsol\cdot X(SAN, insol)}{m\cdot Y(SAN)\cdot C}$$

$$\text{d)GD} = \frac{m\cdot Øinsol\cdot X(SAN, insol)}{[m\cdot Øinsol\cdot X(PB,\ insol)] + [m\cdot Øsol\cdot X(PB,\ sol)]} \text{GE} = \frac{m\cdot Øinsol\cdot X(SAN, insol)}{[m\cdot Øinsol\cdot X(SAN,\ insol)] + [m\cdot Øsol\cdot X(SAN,\ sol)]}$$

where m is the total mass of the sample and C is the overall conversion of the SAN copolymer, Ø sol and Ø insol are the soluble and insoluble fractions of the polymer in the sample, Y (PB), Y (SAN) and Y (NPS) are the fractions of polybutadiene, styrene-acrylonitrile and non-polymerizable solids in the sample and X (SAN, sol), X (SAN, insol) and X (PB, insol) are the fractions of free SAN in the soluble fraction, grafted SAN in the insoluble fractions and polybutadiene in the insoluble fraction of the polymer. Method c) uses X (SAN, insol) from ATR-FTIR and in method d) all fractions are from NMR.

a good compromise can be to use method c) analyzing the insoluble fraction by NMR that does not need a calibration.

CRediT authorship contribution statement

Ainara Agirre: Conceptualization, Formal analysis, Writing – original draft, Writing – review & editing. **Miren Aguirre:** Conceptualization, Formal analysis, Writing – original draft, Writing – review & editing. **Jose R. Leiza:** Conceptualization, Formal analysis, Writing – original draft, Writing – review & editing, All authors certify that they have participated sufficiently in the work to take public responsibility for the content, including participation in the concept, design, analysis, writing, or revision of the manuscript.

Declaration of competing interest

The authors declare that they have no known competing financial interests or personal relationships that could have appeared to influence the work reported in this paper.

Acknowledgments

Financial support from the company Elix Polymers, S.A. is gratefully acknowledged. Technical and human support provided by I. Razkin and Prof. L. Irusta (POLYMAT, UPV/EHU) for ATR-FTIR facilities and for the analysis and discussion are gratefully acknowledged. The author also thank for technical and human support provided by SGiker (UPV/EHU/ERDF, EU), especially to Dr. J.I. Santos and Dr. J.I. Miranda for NMR facilities and for analysis and critical discussion.

Appendix A. Supplementary data

Supplementary data to this article can be found online at https://doi.org/10.1016/j.polymer.2022.124997.

References

[1] D.M. Kulich, S.K. Gaggar, V. Lowry, Stepien, Acrylonitrile-Butadiene-styrene polymers, in: Encyclopedia of Polymer Science and Technology, vol. 1, Copyright John Wiley & Sons, Inc, 2001, pp. 174–203.
[2] X.F. Xu, R. Wang, Z.Y. Tan, et al., Effects of polybutadiene-g-SAN impact modifiers on the morphology and mechanical behaviors of ABS blends, Eur. Polym. J. 41 (8) (2005) 1919–1926.
[3] S.L. Sun, X.Y. Xu, Z.Y. Tan, et al., Effect of ABS grafting degree and compatibilization on the properties of PBT/ABS blends, J. Polym. Sci. 102 (2007) 5363–5371.
[4] N. Zhang, X.X. Bao, Z.Y. Tan, et al., Morphology and mechanical properties of ABS blends prepared from emulsion-polymerization PB-g-SAN impact modifier with AIBN as initiator, J. Appl. Polym. Sci. 105 (2007) 1237–1243.
[5] D. Gesner, Phase separation of some acrylonitrile-butadiene-styrene resins, J. Polym. Sci.: Polym. Chem. 3 (1965) 3825–3831.
[6] G. Riess, J.L. Locatelli, Grafting kinetics in the case of ABS, Adv. Chem. 142 (1975) 186–191.
[7] B. Chauvel, J.C. Daniel, Analytical study of ABS copolymers using a preparative ultracentrifuge, Adv. Chem. 142 (1975) 159–1714.
[8] T. Ricco, A. Pavan, F. Danusso, Dynamic transition of grafted polybutadiene in ABS resins, Polymer 16 (3) (1975) 3–7.
[9] M. Rink, T. Ricco, W. Lubert, A. Pavan, Force-displacement evaluation of macromolecular materials in flexural impact tests. II. Influence of rubber content, degree of grafting, and temperature on the impact behavior of ABS resins, Res. J. Appl. Sci. 22 (1978) 429–443.
[10] E.S. Daniels, V.L. Dimonie, Preparation of ABS (Acrylonitrile/Butadiene/Styrene) latexes using hydroperoxide redox initiators, Res. J. Appl. Sci. 41 (1990) 2463–2477.
[11] M. Bertin, G. Marin, J. Montfort, Viscoelastic properties of acrylonitrile-butadiene-styrene (ABS) polymers in the molten state, Polym. Eng. Sci. 35 (77) (1995).
[12] S. Sohn, S. Kim, I.H. Sung, Synthesis and application of poly(butadiene-g-acrylonitrile-styrene) core-shell rubber particles for use in epoxy resin toughening. I. Synthesis of poly(butadiene-g-acrylonitrile-styrene), J. Appl. Polym. Sci. 61 (1996) 1259–1264.
[13] R. Hu, V.L. Dimonie, Preparation and characterization of poly(butadiene-stat-styrene)/poly(styrene-stat-acrylonitrile) structured latex particles, J. Appl. Polym. Sci. 64 (6) (1997) 1123–1134.
[14] M. Okaniwa, M. Suzuki, Grafted stock synthesis of ABS at the ultimate high ratio of polybutadiene to poly (styrene-co-acrylonitrile), J. Appl. Polym. Sci. 81 (2001) 3462–3470.
[15] H.N. Hipps, G.W. Poehlein, F.J. Schork, Developing a continuous emulsion pBD-graft SAN polymerization process: factors impacting morphology control, Polym. React. Eng. 9 (2) (2015) 37–41.
[16] L. Zhang, S. Sun, X. Ma, et al., Influence of the tert-dodecyl mercaptan content in poly(acrylonitrile-butadiene-styrene) on properties of chlorinated polyvinyl chloride/poly(acrylonitrile-butadiene-styrene) blends, Polym. Eng. Sci. 52 (4) (2012) 820–825.
[17] R. Kuhn, H.G. Müller, G. Bayer, et al., Characterization of bimodal bigraft ABS, Colloid Polym. Sci. 271 (2) (1993) 133–142.
[18] A. Zamani, F. Abbasi, A.M. Agah, Characterization of rubber phase in acrylonitrile-butadiene-styrene polymers, J. Appl. Polym. Sci. 114 (2009) 1908–1913.
[19] F. Abbasi, A.M. Agah, E. Mehravar, Study of the effective process parameters influencing styrene and acrylonitrile grafting onto seeded polybutadiene latex, J. Appl. Polym. Sci. 119 (2011) 1752–1761.
[20] F.S. Parker, Quantitative analysis, in: Applications of Infrared Spectroscopy in Biochemistry, and Medicine, Springer, 1971, pp. 80–83.
[21] C. Plessis, G. Arzamendia, J.R. Leiza, et al., Seeded semibatch emulsion polymerization of butyl acrylate: effect of the chain-transfer agent on the kinetics and structural properties, Macromolecules 33 (2000) 5041–5047.
[22] A. Agirre, J.I. Santos, J.R. Leiza, Toward understanding the architecture (branching and MWD) of crosslinked acrylic latexes, Macromol. Chem. Phys. 214 (2013) 589–598.
[23] P. Castignolles, R. Graf, M. Parkinson, M. Wihelm, M. Gaborieau, Detection and quantification of branching in polyacrylate by size-exclusion chromatography (SEC) and melt-state ^{13}C NMR spectroscopy, Polymer 50 (11) (2009) 2373–2383.